

1 **Low immunogenicity of malaria pre-erythrocytic stages can be overcome by**
2 **vaccination**

3

4

5 Katja Müller^{1,2,†}, Matthew P. Gibbins^{3,†}, Arturo Reyes-Sandoval⁴, Adrian V. S. Hill⁴, Simon J.
6 Draper⁴, Kai Matuschewski^{1,2}, Olivier Silvie⁵ & Julius Clemence R. Hafalla^{3,*}

7

8 ¹Parasitology Unit, Max Planck Institute for Infection Biology, Berlin, Germany.

9 ²Molecular Parasitology, Institute of Biology, Humboldt University, Berlin, Germany.

10 ³Department of Immunology and Infection, Faculty of Infectious and Tropical Diseases,
11 London School of Hygiene and Tropical Medicine, London, United Kingdom.

12 ⁴Jenner Institute, University of Oxford, Old Road Campus Research Building, Oxford, United
13 Kingdom.

14 ⁵Sorbonne Université, INSERM, CNRS, Centre d'Immunologie et des Maladies
15 Infectieuses, CIMI-Paris, Paris, France.

16 † Contributed equally to this work

17 * Corresponding author: Julius.Hafalla@lshtm.ac.uk

18

19

20 **Keywords:** malaria, *Plasmodium*, antigen, vaccine, immunogenicity, protective efficacy,
21 sporozoite, liver stage.

22

23 **ABSTRACT**

24 Vaccine discovery and development critically depends on predictive assays, which prioritise
25 protective antigens. Immunogenicity is considered one important criterion for progression of
26 candidate vaccines to further clinical evaluation, including phase I/II trials. Here, we tested
27 this assumption in an infection and vaccination model for malaria pre-erythrocytic stages.
28 We engineered *Plasmodium berghei* parasites that harbour a well-characterised epitope for
29 stimulation of CD8⁺ T cells either as an antigen in the circumsporozoite protein (CSP), the
30 surface coat protein of extracellular sporozoites or in the upregulated in sporozoites 4
31 (UIS4), a major protein associated with the parasitophorous vacuole membrane (PVM) that
32 surrounds the intracellular exo-erythrocytic forms (EEF). We show that the antigen origin
33 results in profound differences in immunogenicity with a sporozoite antigen eliciting robust
34 and superior antigen-specific CD8⁺ T cell responses, whilst an EEF antigen evokes poor
35 responses. However, despite their contrasting immunogenic properties, both sporozoite and
36 EEF antigens gain access to antigen presentation pathways in hepatocytes, as recognition
37 and targeting by vaccine-induced, antigen-specific effector CD8⁺ T cells results in high
38 levels of protection when targeting both antigens. Our study is the first demonstration that
39 poor immunogenicity of EEF antigens does not preclude their susceptibility to antigen-
40 specific CD8⁺ T cell killing. Our findings that antigen immunogenicity is an inadequate
41 predictor of vaccine susceptibility have wide-ranging implications on antigen prioritisation for
42 the design and testing of next-generation pre-erythrocytic malaria vaccines.

43 INTRODUCTION

44 Malaria, caused by the apicomplexan parasites *Plasmodium*, is responsible for 228
45 million clinical cases and 405,000 deaths annually worldwide¹. Whilst current malaria control
46 strategies have led to marked reduction in incidence rate, cases, and mortality for the past
47 16 years, a highly efficacious vaccine is likely essential to approach the ambitious World
48 Health Organisation's (WHO) vision of "a world free of malaria". Targeting the malaria pre-
49 erythrocytic stages, an obligatory and clinically silent phase of the parasite's life cycle, is
50 considered an ideal and attractive strategy for vaccination; inhibiting parasite infection of and
51 development in hepatocytes results in preclusion of both disease-causing blood stages and
52 transmissible sexual stages. Yet, despite intensive research for over 25 years, a highly
53 efficacious pre-erythrocytic stage vaccine remains elusive². An in-depth characterisation of
54 how the complex biology of pre-erythrocytic stages influences the generation and protective
55 efficacy of immune responses is warranted to inform the design of future malaria vaccines.

56 CD8+ T cells are crucial mediators of protective immunity to malaria pre-erythrocytic
57 stages³. Whilst often considered as a single phase of the parasite's life cycle, the malaria
58 pre-erythrocytic stage is comprised of two different parasite forms: (i) sporozoites, which are
59 motile extracellular parasites that are delivered by infected mosquitoes to the mammalian
60 host, and (ii) exo-erythrocytic forms (EEF; also known as liver stages), which are intracellular
61 parasites resulting from the differentiation and growth of sporozoites inside a
62 parasitophorous vacuole (PV) within hepatocytes⁴. How these two spatially different parasite
63 forms and the ensuing temporal expression of parasite-derived antigens impact the
64 magnitudes, kinetics and phenotypes of CD8+ T cell responses elicited following infection is
65 poorly understood. Furthermore, the complexity within the pre-erythrocytic stages has fuelled
66 a long-standing debate focused on the contributions of distinct sporozoite and EEF antigens
67 in parasite-induced responses, and whether sporozoite or EEF proteins are better targets of
68 vaccines.

69 Our current understanding of CD8+ T cell responses to malaria pre-erythrocytic
70 stages has been largely based on measuring responses to the H-2-K^d-restricted epitopes of
71 *P. yoelii* (*Py*)⁵ and *P. berghei* (*Pb*)⁶ circumsporozoite proteins (CSP), the major surface

72 antigen of sporozoites. Many of these fundamental studies have focused on using infections
73 with irradiated sporozoites, the gold-standard vaccine model for malaria. Infection with *Py*
74 sporozoites elicits an expected T cell response typified by early activation and induction of
75 effector CSP-specific CD8+ T cells followed by contraction and establishment of quantifiable
76 memory populations⁷. CSP-specific CD8+ T cells are primed by dendritic cells that cross-
77 present sporozoite antigens via the endosome-to-cytosol pathway⁸. Yet, CSP is a unique
78 antigen because it is expressed in both sporozoites and EEFs⁹. Whilst the expression of
79 CSP mRNA ceases after sporozoite invasion, the protein on the parasite surface is stable
80 and endures in EEFs during development in hepatocytes¹⁰. *In vitro* data indicate that primary
81 hepatocytes process and present *Pb*CSP-derived peptides to CD8+ T cells in a proteasome-
82 dependent manner, involving export of antigen to the cytosol⁸. Taken together, these data
83 imply that sporozoite antigens induce quantifiable CD8+ T cell responses after infection.
84 Antigens that have similar expression to the CSP, persisting to EEFs and with epitope
85 determinants presented on hepatocytes, are excellent targets of CD8+ T cell-based
86 vaccines.

87 The paucity of EEF only-specific epitopes has hindered not only our ability to
88 understand the immune responses that are evoked whilst the parasite is in the liver, but also
89 their utility as targets of vaccination. Accordingly, the contribution of EEF-infected
90 hepatocytes in the *in vivo* induction of CD8+ T cell responses is poorly understood. The liver
91 is an organ where the primary activation of CD8+ T cells is generally biased towards the
92 induction of tolerance^{11,12}. Yet, studies in other model systems have demonstrated antigen-
93 specific primary activation within the liver¹³. Another confounding issue with EEFs is their
94 development in PVs with constrained access to the hepatocyte's cytosol⁴. Nonetheless, if
95 CD8+ T cells specific for EEF antigens are primed, do they expand and contract with distinct
96 kinetics? Moreover, are EEF-specific epitopes efficiently generated for recognition and
97 targeting by vaccine-induced CD8+ T cells? Answers to these questions will be key for
98 antigen selection and design of future malaria vaccines.

99 In this study, we compared the initiation and development of CD8+ T cell responses
100 – elicited following parasite infection – to CSP, a sporozoite antigen, and to upregulated in

101 infective sporozoites gene 4 (UIS4), an EEF-specific vacuolar protein¹⁴. UIS4, a member of
102 the early transcribed membrane protein (ETRAMP) family, is abundantly expressed in EEFs
103 and associates with the PVM¹⁴. Whilst UIS4 mRNA expression is present in sporozoites,
104 translation is repressed until when EEFs develop¹⁰. To control for epitope specificity, we
105 generated *Pb* transgenic parasites that incorporate the H-2-K^b epitope SIINFEKL, from
106 ovalbumin, in either CSP or UIS4. Furthermore, we evaluated the capacity of vaccine-
107 induced CD8+ T cells to target these parasites in a mouse challenge model. Our data show
108 disparate immunogenic properties between a sporozoite and an EEF vacuolar membrane
109 antigen but equivalent susceptibility to vaccine-induced CD8+ T cells.

110 RESULTS

111 Transgenic CSP^{SIINFEKL} and UIS4^{SIINFEKL} parasites display normal sporozoite motility 112 and liver invasion

113 We generated, by double homologous recombination, transgenic *Pb* parasites
114 expressing the immunodominant H-2-K^b-restricted CD8+ T cell epitope of ovalbumin
115 (SIINFEKL) in the context of the sporozoite surface antigen CSP or the EEF vacuolar
116 membrane antigen UIS4 (**Figure 1a and Supplementary Figure 1a, b**). Constructs included
117 the *TgDHFR/TS* positive selection cassette and incorporated SIINFEKL in the context of the
118 gene open reading frame. For CSP^{SIINFEKL}, SIINFEKL replaced SYIPSAEKI, the
119 immunodominant H-2-K^d-restricted CD8+ T cell epitope of CSP, which allowed for
120 recognition in H-2-K^b-carrying C57BL/6 mice. For UIS4^{SIINFEKL}, the SIINFEKL epitope was
121 added to the immediate C-terminus of the UIS4 protein. Appending the C-terminus was
122 chosen because it had been shown in *Toxoplasma gondii* that the potency of the
123 immunodominant epitope of GRA6 was associated with its C-terminal location, which may
124 have enhanced the presentation by parasite-infected cells¹⁵. Whilst undefined for UIS4 itself,
125 it has been shown for several other ETRAMPs that the C-terminus faces the host cell
126 cytoplasm¹⁶, which might enhance exposure to the MHC I machinery.

127 The resulting parasites showed a phenotype comparable to WT parasites, with
128 functional sporozoite motility (**Figure 1b**) and normal invasive capacity and development
129 inside hepatocytes (**Figure 1c**), as well as comparable midgut infectivity and number of
130 salivary gland sporozoites (**Supplementary Figure 1c, d**). Thus, the introduced mutations to
131 generate CSP^{SIINFEKL} and UIS4^{SIINFEKL} parasites did not interfere with the completion of the
132 life cycle, in either mosquito vector or mouse. All C57BL/6 mice that received 800
133 sporozoites of either CSP^{SIINFEKL} or UIS4^{SIINFEKL} intravenously developed a patent blood
134 stage infection by day 4, comparable to infection with WT sporozoites (data not shown).

135

136 Peripheral blood CD8+ T cell responses and early proliferative capacity of splenic 137 CD8+ T cells are superior if elicited by a sporozoite surface protein in contrast to a 138 vacuolar membrane protein in the infected liver

139 We first wanted to determine whether the generated transgenic parasites allow
140 antigen-specific responses to be tracked using SIINFEKL as a surrogate CD8+ T cell
141 epitope for sporozoite surface and EEF vacuolar membrane antigens. To this end, we
142 assessed the kinetics of the CD8+ T cell response following intravenous immunisation with
143 CSP^{SIINFEKL} or UIS4^{SIINFEKL} sporozoites. To augment the CD8+ T cell response, mice were
144 adoptively transferred with 2×10^6 OT-I cells expressing a SIINFEKL-specific TCR⁸, prior to
145 receiving 10,000 γ -radiation attenuated WT, CSP^{SIINFEKL} or UIS4^{SIINFEKL} sporozoites. Prior
146 work showed that γ -radiation attenuation of *P. berghei* sporozoites does not impact host cell
147 invasion and UIS4 expression¹⁷.

148 Peripheral blood was taken at days 4, 7, 14, 21, 42 and 88 after immunisation and
149 CD8+ T cell responses were analysed after staining with H-2-K^b-SIINFEKL pentamers and
150 for CD11a, a marker for antigen-experienced T cells^{18,19} (**Figure 2a**). A substantial
151 proportion of K^b-SIINFEKL+ CD11a+ CD8+ T cells were observed in mice immunised with
152 CSP^{SIINFEKL}; the response was highest on day 4, reaching 5% of all antigen-experienced
153 CD8+ T cells, and declined steadily until day 21, when the response stabilised and remained
154 unchanged for several weeks (**Figure 2b**). In marked contrast, UIS4^{SIINFEKL} immunisation
155 induced a poor CD8+ T cell response; the proportion of K^b-SIINFEKL+ CD11a+ CD8+ T
156 cells was only higher than the control groups at day 4 after immunisation, and the response
157 remained within background levels for the duration of the experiment. Control groups
158 included mice receiving OT-I cells only or in addition to WT sporozoites, which lack
159 SIINFEKL sequences.

160 The poor CD8+ T cell response induced by UIS4^{SIINFEKL} sporozoites, as compared to
161 CSP^{SIINFEKL}, led us to characterise the early events in the proliferation and differentiation of
162 these cells. Mice were adoptively transferred with CFSE-labelled OT-I cells and immunised
163 with γ -radiation attenuated WT, CSP^{SIINFEKL} or UIS4^{SIINFEKL} sporozoites. As shown by gating
164 on CD8+ T cells (**Figure 2c, g**), after 5 days, immunisation with CSP^{SIINFEKL} sporozoites
165 recruited K^b-SIINFEKL+ CD8+ T cells to undergo massive proliferative activity, which was 6x
166 larger than that observed with UIS4^{SIINFEKL} sporozoites, in good agreement with the
167 peripheral blood data described above (**Figure 2b**). Consistent with the activation of these

168 cells, the proliferation of antigen-specific CD8⁺ T cells by both parasites was associated with
169 the development of effector and effector-memory phenotypes as evidenced by upregulation
170 of CD11a and CD49d, and downregulation of CD62L, respectively (**Figure 2d-f**).

171 Taken together, these findings establish that immunisations with CSP^{SIINFEKL} and
172 UIS4^{SIINFEKL} sporozoites permit antigen-specific responses to be tracked longitudinally in the
173 peripheral blood. Importantly, we demonstrate that a sporozoite surface protein evokes a
174 CD8⁺ T cell response of superior magnitude than an EEF vacuolar membrane protein
175 following immunisation with malaria sporozoites.

176

177 **High magnitude splenic and hepatic CD8⁺ T cell responses to a sporozoite antigen**

178 Previous research has shown that CD8⁺ T cells are primed primarily in the spleen
179 following intravenous immunisation with malaria sporozoites²⁰ and that liver lymphocytes
180 form a front-line defence against developing EEFs in hepatocytes^{21,22}. Thus we further
181 analysed the development of CD8⁺ T cell responses in the spleens and livers of mice
182 adoptively transferred with OT-I cells and intravenously immunised with WT, CSP^{SIINFEKL} or
183 UIS4^{SIINFEKL} sporozoites. Consistent with our aforementioned results, surface staining of
184 splenic and liver lymphocytes showed higher proportion and absolute numbers of K^b-
185 SIINFEKL⁺ CD11a⁺ CD8⁺ T cells at day 14 and day 42 following immunisation with
186 CSP^{SIINFEKL} compared to UIS4^{SIINFEKL} sporozoites (**Figure 3a-c**). In addition to CD11a
187 upregulation, the splenic and liver CD8⁺ T cells, elicited by both CSP^{SIINFEKL} or UIS4^{SIINFEKL}
188 sporozoites, had effector and effector memory cell phenotypes (CD62L⁻, CD49d⁺ and
189 CD44⁺) (**Supplementary Figure 2**). Although low, the numbers of antigen-specific CD8⁺ T
190 cells induced by UIS4^{SIINFEKL} sporozoites were within the detection limits of the assay.

191 To assess for effector functions, splenic and liver lymphocytes were stimulated *ex*
192 *vivo* with the SIINFEKL peptide. Generally, higher numbers (proportion and absolute
193 numbers) of IFN- γ -secreting CD8⁺ T cells were observed at day 14 and day 42 following
194 immunization with CSP^{SIINFEKL} compared to UIS4^{SIINFEKL} sporozoites (**Figure 3d-f**). In
195 addition, these CD8⁺ T cells also expressed TNF and IL-2, suggesting some potential
196 polyfunctionality (**Supplementary Figure 3**).

197 Altogether, even though effector and effector memory CD8⁺ T cell responses can be
198 detected against both sporozoite surface protein and EEF vacuolar membrane protein
199 antigens following immunisation with malaria sporozoites, the two antigens show a striking
200 difference in the magnitude of CD8⁺ T cell responses they induce.

201

202 **Quantification of endogenously produced antigen-specific CD8⁺ T cells following** 203 **intravenous or intradermal parasite immunisation**

204 Previous work tracking responses to SIINFEKL-tagged proteins has used adoptively
205 transferred cells from OT-I mice, with all T cells from these mice expressing T cell receptors
206 specific to SIINFEKL^{8,23}. We employed this robust approach by adoptively transferring a
207 fixed amount of OT-I splenocytes in order to augment the response and allow visualisation
208 **(Figures 2 and 3)**. Next, we wanted to explore whether we can capture the endogenous K^b-
209 SIINFEKL⁺ CD11a⁺ CD8⁺ T cell population, which is elicited by immunising with parasites
210 without OT-I cell transfer. We performed *ex vivo* restimulation of lymphocytes with SIINFEKL
211 peptide followed by flow cytometry and were able to clearly identify the endogenous
212 population with a trend complementary to our earlier results **(Figure 4a-c)**. Immunisation
213 with CSP^{SIINFEKL} sporozoites elicited a superior splenic and liver CD8⁺ T cell response than
214 with UIS4^{SIINFEKL} sporozoites. As expected, the proportion and absolute cell numbers were
215 considerably lower than with adoptive transfer of OT-I cells, but this did not preclude the
216 ability to visualise IFN- γ -secreting CD8⁺ T cells and capture the differences between the two
217 groups.

218 Under normal conditions of transmission, sporozoites are delivered into the host skin
219 by mosquito bite. All preceding immunisation experiments were performed with parasites
220 injected intravenously. As a proxy for the natural route of infection, whilst ensuring consistent
221 quantities of parasites were inoculated, CSP^{SIINFEKL} and UIS4^{SIINFEKL} sporozoites were
222 injected via the intradermal route into the ear pinnae. Under these conditions, CSP still
223 induced a greater number of IFN- γ -secreting SIINFEKL-specific CD8⁺ T cells following
224 restimulation with SIINFEKL compared to UIS4, with a comparable magnitude as after
225 intravenous injection **(Figure 4d-f)**. Thus, these biologically and immunologically more

226 appropriate data entirely recapitulate the strong immunogenicity of a sporozoite surface
227 antigen compared to an EEF vacuolar membrane protein.

228

229 **Increasing the amount of EEF vacuolar membrane antigen does not impact its**
230 **immunogenicity.**

231 Both CSP and UIS4 are critical proteins expressed by the sporozoite and EEF
232 respectively, and both proteins are important for survival and succession into the subsequent
233 life stage and parasite form^{10,14,24}. Previous studies have shown that the magnitude of the
234 CD8+ T cell response to a sporozoite surface antigen depended on the amount of parasites
235 used for immunisation²⁵. Hence, poor immunogenicity of an EEF vacuolar membrane protein
236 could be a result of the lower level of protein expression during parasite infection. It is
237 possible to enhance CD8+ T cell responses by increasing the number of parasites used for
238 immunisation²⁵. Therefore, we immunised groups of mice with 8,000 CSP^{SIINFEKL}, 8,000
239 UIS4^{SIINFEKL} or 64,000 UIS4^{SIINFEKL} sporozoites and compared the magnitude of the elicited
240 antigen-specific responses. Strikingly, the CD8+ T cell response following 8x sporozoite
241 immunisation dose with UIS4^{SIINFEKL} did not increase proportionally and was not significantly
242 higher than immunisation with a 1x dose (**Figure 5a, b**). This result suggests that, in the
243 context of attenuated sporozoite immunisation, EEF vacuolar membrane antigens are poorly
244 immunogenic and increasing antigen fails to substantially improve the magnitude of CD8+ T
245 cell responses.

246

247 **Immunogenicity of parasite antigens does not predict effector responses following**
248 **vaccination**

249 Our findings thus far showed that sporozoite surface proteins appear more
250 immunogenic than EEF vacuolar membrane proteins and raised an intriguing and important
251 question; does immunogenicity predict susceptibility to vaccine-induced effector responses?
252 To address this, we vaccinated mice, which had received OT-I cells, with a recombinant
253 adenovirus expressing full-length ovalbumin²⁶. This vaccination protocol resulted in
254 frequencies of ~7.5% SIINFEKL-specific CD8+ T cells in peripheral blood (**Figure 6a, b**).

255 Vaccinated mice were then challenged with CSP^{SIINFEKL} or UIS4^{SIINFEKL} sporozoites, and
256 protection was assessed 19 days after vaccination by two complementary assays; (i)
257 determination of the reduction of parasite load in the liver 42 hours after sporozoite
258 challenge (**Figure 6c**), and (ii) induction of sterile protection (**Figure 6d**). Vaccinated mice
259 challenged with CSP^{SIINFEKL} or UIS4^{SIINFEKL} sporozoites showed a dramatic reduction in
260 parasite load in the liver (**Figure 6c**) as compared to vaccinated mice challenged with WT
261 parasites. Strikingly, there was no statistical difference in the protection observed when
262 vaccinated mice were challenged with either CSP^{SIINFEKL} or UIS4^{SIINFEKL} sporozoites.
263 Consistent with these findings, both groups of vaccinated mice challenged with either
264 CSP^{SIINFEKL} or UIS4^{SIINFEKL} sporozoites exhibited sterile protection of comparable levels
265 (**Figure 6d**). These findings indicate that spatial and temporal aspects of antigen expression
266 may affect protein immunogenicity in the context of parasitic infection but not necessarily the
267 same target's susceptibility for antigen-specific CD8+ T cell killing.
268

269 DISCUSSION

270 The malaria pre-erythrocytic stages have been a prime target for the development of
271 a *Pf* vaccine for more than 35 years. Indeed, RTS,S/AS01, the most advanced malaria sub-
272 unit vaccine candidate to date is based on CSP, the major surface protein of sporozoites²⁷.
273 Yet, final results of the Phase III trial showed that RTS,S/AS01 offers only modest efficacy,
274 which rapidly wanes over time²⁸. Thus, there is an imperative need not only to widen the
275 pursuit for new sub-unit vaccine candidates, but also to radically improve the antigen
276 selection process. Antigens are generally prioritised based on a range of criteria, including
277 their immunogenicity in the context of parasitic infection. We examined this notion in an
278 infection and vaccination model for malaria pre-erythrocytic stages.

279 The malaria pre-erythrocytic stages consist of two spatially-different parasite forms:
280 extracellular sporozoites and intracellular EEFs. The transformation of sporozoites into EEFs
281 involves regulation at both transcriptional²⁹ and translational^{30,31} levels, resulting in both the
282 spatial and temporal expression of many antigens that are distinct for each parasite form³².
283 Whilst our current understanding of immune responses to malaria pre-erythrocytic stages
284 has focused on CSP, the lack of well-defined epitopes that are expressed only by EEFs has
285 restrained fundamental studies investigating the contributions of EEF antigens in parasite-
286 induced CD8+ T cell responses and their value as target of vaccines.

287 In this study, we contrasted the development of CD8+ T cell responses induced by
288 CSP and UIS4, two major proteins expressed by sporozoites and EEFs, respectively. We
289 generated transgenic *Pb* parasites where SIINFEKL is expressed as part of either CSP or
290 UIS4, allowing the presentation of the epitope at the same space and time as the respective
291 protein. This approach is in contrast to a more common strategy of expressing the whole, or
292 a fragment of, ovalbumin inserted as a transgene into the *Pb* genome, and then tracking the
293 immune response elicited by an extraneous molecule^{23,33}. Since CSP is expressed in both
294 sporozoites and EEFs, the processing and presentation of the SIINFEKL in CSP^{SIINFEKL}
295 occurs as soon as sporozoites are inoculated and are able to interact with dendritic cells,
296 which present antigens via an endosome-to-cytosol pathway⁸; CSP also has direct access to
297 the hepatocyte's cytosol for processing and presentation of the CSP-derived epitope⁸.

298 However, since UIS4 is expressed only in the PVM of EEFs, processing and presentation of
299 the epitope in UIS4^{SIINFEKL} is restricted to just hepatocytes.

300 Our results establish that following sporozoite-immunisation, a sporozoite surface
301 protein induces superior CD8+ T cell responses – as measured both by pentamer staining
302 and by IFN- γ secretion following peptide stimulation – than an EEF vacuolar membrane
303 protein. Detailed kinetic and phenotypic analysis of the development of antigen-specific
304 CD8+ T cells to both CSP and UIS4 revealed that the responses differ in magnitude,
305 demonstrating the ability of both antigens to elicit effector and effector memory responses.
306 There was no difference in our results whether sporozoites are delivered using the
307 commonly used intravenous immunisation or the more physiological intradermal delivery.
308 We also showed that increasing the number of UIS4^{SIINFEKL} parasites used for immunisation
309 did not augment CD8+ T cell responses, signifying that the poor immunogenicity of an EEF
310 vacuolar membrane protein is not due to the level of UIS4 expression during parasite
311 infection. Our findings support the idea that EEF antigens have minimal contributions to the
312 magnitude of immune responses following whole sporozoite immunisation, which
313 corroborates with prior data showing that that hepatocytes are poor at priming T cell
314 responses^{11,12}.

315 Regardless of their differing immunogenicities in the context of parasitic infection, we
316 further demonstrated that both sporozoite and EEF antigens are effectively targeted by
317 antigen-specific effector CD8+ T cells, which were generated by vaccination using priming
318 and boosting with recombinant viruses expressing the epitope. Importantly, mice harbouring
319 vaccine-induced, antigen-specific CD8+ T cells were comparably protected when challenged
320 with either CSP^{SIINFEKL} or UIS4^{SIINFEKL}. These findings imply that both sporozoite and EEF
321 antigens comparably access the antigen presentation pathways in hepatocytes leading to
322 recognition of defined epitopes.

323 Our study is the first demonstration that poor natural immunogenicity, in this case of
324 an EEF antigen, does not preclude antigen-specific CD8+ T cell killing. Our findings that
325 antigen immunogenicity in this context is an inadequate predictor of vaccine efficacy have
326 wide-ranging implications on antigen prioritisation for the design and testing of next-

327 generation pre-erythrocytic malaria vaccines. Thus, the strategy to screen for T cell
328 responses in naturally infected or sporozoite-immune volunteers to prioritise vaccine
329 candidates requires some form of reassessment. It is noteworthy that for other stages of
330 malaria infection, antigens that give limited or no responses e.g. RH5^{34,35} and sexual stage
331 antigens³⁶, are promising antibody targets for vaccines.

332 A key direction for future research will be identifying the mechanisms by which EEF
333 antigens elicit protection and finding new assays to easily distinguish good vaccine targets,
334 namely those antigens that can protect (via susceptibility to vaccine-induced CD8+ T cells),
335 rather than those that naturally induce strongly immunogenic responses. Ultimately, the
336 molecular mechanisms of presentation of EEF antigens, those expressed in the PVM and
337 within the parasite itself, onto the surface of infected hepatocytes remains to be fully
338 understood. Determination of the processes involved in parasite antigen presentation in the
339 pre-erythrocytic stages of malaria may elucidate links to protection and the identification of
340 further antigens that could drive the development of an efficacious protective malaria
341 vaccine.

342

343 **METHODS**

344 **Ethics and animal experimentation**

345 Animal procedures were performed in accordance with the German
346 'Tierschutzgesetz in der Fassung vom 18. Mai 2006 (BGBl. I S. 1207)' which implements the
347 directive 2010/6 3/EU from the European Union. Animal experiments at London School of
348 Hygiene and Tropical Medicine were conducted under license from the United Kingdom
349 Home Office under the Animals (Scientific Procedures) Act 1986. NMRI, CD-1, C57BL/6 and
350 OT-I laboratory mouse strains were bred in house at LSHTM or purchased from Charles
351 River Laboratories (Margate, UK or Sulzfeld, Germany). Female mice were used for
352 experiments at the age of 6-8 weeks.

353

354 **Generation of transgenic parasites**

355 Transgenic *P. berghei* ANKA mutants CSP^{SIINFEKL} and UIS4^{SIINFEKL} were developed
356 using double homologous recombination. In the CSP^{SIINFEKL} mutant, the CSP gene is altered
357 so the epitope SYIPSAEKI (residues 252-260) is replaced with the H-2^b restricted *Gallus*
358 *gallus* ovalbumin epitope SIINFEKL. In the UIS4^{SIINFEKL} mutant, the SIINFEKL epitope is
359 appended to the C-terminal end of the UIS4 protein. Clonal parasite lines were generated by
360 limiting dilution. Details of plasmid design, including the primers used and the cloning of
361 parasites can be found in Supplementary Experimental Procedures and Table S1.

362

363 ***Plasmodium berghei* ANKA immunisation**

364 *P. berghei* wild type (WT; strain ANKA clone c15cy1 or clone 507) parasites and
365 CSP^{SIINFEKL} and UIS4^{SIINFEKL} (clone c15cy1) parasites were maintained by continuous cycling
366 between murine hosts (NMRI or CD-1) and *Anopheles stephensi* mosquitoes. Infected
367 mosquitoes were kept in incubators (Panasonic and Mytron) at 80% humidity and 20°C.
368 Sporozoites were isolated from salivary glands and γ -irradiated at 1.2×10^4 cGy. Mice were
369 immunised intravenously in the lateral tail vein or intradermally in the ear pinnae with 10,000
370 sporozoites, unless otherwise stated, and challenged with either 1,000 or 10,000 sporozoites
371 injected intravenously.

372

373 **Indirect fluorescent antibody staining (IFA) of sporozoites**

374 Epoxy-covered 8-well glass slides were coated with 3% BSA-RPMI. 10,000
375 sporozoites were added per well in 3% BSA-RPMI and incubated for 45 minutes during
376 which the shed surface proteins are deposited in the gliding motility process. Sporozoites
377 and their trails were stained with a mouse anti-CSP³⁷ primary antibody and a rabbit
378 polyclonal anti-*PbUIS4*³⁰ primary antibody and the respective fluorescently labelled
379 secondary antibodies. Nuclei were stained with Hoechst 33342 and slides mounted with
380 'Fluoromount-G' (Southern Biotech). Sporozoites and trails were analysed by fluorescent
381 microscopy (Zeiss Axio Observer).

382

383 ***In vitro* infection of hepatoma cells and fluorescent staining**

384 *In vitro* EEF development was analysed in infected Huh7 hepatoma cells for 24 and
385 48 hours. Triplicate Labtek (Permanox plastic - Nunc) wells were infected with 10,000
386 transgenic CSP^{SIINFEKL} or UIS4^{SIINFEKL} parasites and duplicate wells were infected with 10,000
387 WT parasites. Infected cells were analysed by fluorescence microscopy using a mouse anti-
388 *PbHSP70*³⁸ and a rabbit polyclonal anti-*PbUIS4*³⁰ primary antibody, the respective
389 fluorescently labelled secondary antibodies and nuclear staining with Hoechst 33342.
390 Stainings were analysed by fluorescent microscopy (Zeiss Axio Observer).

391

392 **Quantification of SIINFEKL-specific CD8+ T cell responses**

393 Spleens and livers were harvested from immunised or naïve mice and perfused with
394 PBS. Lymphocytes were derived from spleens by passing through 40 or 70µm cell strainers
395 (Corning) and from livers by passing through 70µm cell strainers (Corning). Red blood cells
396 were lysed with PharmLyse (BD), and lymphocytes were resuspended in complete RPMI
397 (cRPMI- RPMI + 10% FCS + 2% Penicillin-Streptomycin + 1% L-glutamine (Gibco)). For cell
398 counting, lymphocytes were diluted 40x with Trypan Blue (ThermoFisher Scientific) and
399 enumerated using a Neubauer 'Improved' haemocytometer (Biochrom). Alternatively,
400 lymphocytes were counted using a MACSQuant flow cytometer (Miltenyi Biotec), using

401 propidium iodide (PI) (Sigma Aldrich) or, in the case of hepatic lymphocytes, using CD45.2-
402 Alexa647 (Biolegend) to distinguish between hepatocytes and lymphocytes, prior to PI
403 administration and counting. Peripheral blood was acquired by tail vein puncture collected in
404 Na⁺ heparin capillary tubes (Brand) and assayed in 96-well flat bottom plates (Corning). For
405 CD8⁺ T cell stimulations, 2-3x10⁶ splenocytes or 1-2x10⁵ liver cells were incubated with
406 SIINFEKL peptide (Peptides and Elephants, Henningsdorf) at a final concentration of
407 10µg/ml in the presence of Brefeldin A (eBioScience). Cells were incubated at 37°C, 5%
408 CO₂ for 5-6 hours, before incubation at 4°C overnight. For staining of cell surface markers
409 and intracellular cytokines, cells were incubated for 1 hour at 4°C. Cells derived from the
410 spleen or liver were fixed with 4% paraformaldehyde, and cells from peripheral blood were
411 fixed with 1% paraformaldehyde between the extra- and intracellular staining steps. Data
412 was acquired by flow cytometry using an LSRII or LSRFortessa (BD). Antibodies used for
413 staining were as follows; BD: CD3 (500A2); eBioScience: CD8 (53-6.7), CD11a (M17/4),
414 CD49d (R1-2), CD62L (MEL-14), CD44 (IM7), IFN-γ (XMG1.2), TNF-α (MP6-XT22) and IL-2
415 (JES6-5H4); ProImmune: H-2-K^b-SIINFEKL pentamers.

416

417 **CFSE labelling of OT-I cells**

418 Splens from OT-I mice were lysed and cells washed twice in PBS without serum.
419 Splenocytes resuspended at a density of 5x10⁶ cells/ml in PBS had 1:5,000 CFSE
420 (ThermoFisher Scientific) added and were incubated in the dark at room temperature, with
421 gentle inversion for 4 minutes. The labelling reaction was quenched with cRPMI and cells
422 washed twice in cRPMI. Cells were recounted and 2x10⁶ cells were injected per mouse.

423

424 **Vaccination with OVA expressing recombinant adenovirus**

425 To assess parasite liver load after vaccination with virus-expressed OVA, groups of
426 C57BL/6 mice were immunized with recombinant human adenovirus serotype 5 (AdHu5)
427 expressing full-length chicken ovalbumin²⁶. Each mouse received 1x10⁸ infective units (ifu) in
428 a volume of 100µl administered intramuscularly (50µl into each thigh). At the same time mice
429 received OT-I splenocytes intravenously (2x10⁶ cells/mouse). 19 days after vaccination,

430 vaccinated and naïve control mice were challenged with 10,000 WT, CSP^{SIINFEKL} or
431 UIS4^{SIINFEKL} sporozoites administered intravenously. 42 hours after the challenge the livers
432 were harvested and homogenised in Trizol (ThermoFisher Scientific) for total RNA isolation.
433 Afterwards, cDNA was generated using the RETROScript Kit (Ambion). Quantitative real-
434 time PCR was performed using the StepOnePlus Real-Time PCR System and Power SYBR
435 Green PCR Master Mix (Applied Biosystems). Relative liver parasite levels were quantified
436 using the $\Delta\Delta C_t$ method comparing levels of *P. berghei* 18S rRNA normalised to mouse
437 *GAPDH* mRNA³⁰. To assess sterile protection, AdHu5 OVA-vaccinated and control mice
438 received 2×10^6 OT-I splenocytes one day prior to vaccination. 14 days later, all mice were
439 challenged with 1,000 WT, CSP^{SIINFEKL} or UIS4^{SIINFEKL} sporozoites. Blood smears were taken
440 from day 3-14 after challenge to determine the presence of blood stage parasites.

441

442 **Statistics**

443 Data were analysed using FlowJo version 9.5.3 (Tree Star Inc., Oregon, USA),
444 Microsoft Excel and GraphPad Prism v7 (GraphPad Software Inc., CA, USA). We used
445 Mann-Whitney U test for analysing data that were not normally distributed and Welch's t-test
446 or one-way ANOVA with Tukey's multiple comparison test for normally distributed data.

447

448 **REFERENCES**

- 449 1 WHO. World Malaria Report 2019 (World Health Organisation, Geneva, Switzerland, 2017).
- 450 2 Draper, S. J. *et al.* Malaria Vaccines: Recent Advances and New Horizons. *Cell Host Microbe*
451 **24**, 43-56, doi:10.1016/j.chom.2018.06.008 (2018).
- 452 3 Doolan, D. L. & Hoffman, S. L. The complexity of protective immunity against liver-stage
453 malaria. *Journal of immunology* **165**, 1453-1462 (2000).
- 454 4 Hafalla, J. C., Silvie, O. & Matuschewski, K. Cell biology and immunology of malaria.
455 *Immunological reviews* **240**, 297-316, doi:10.1111/j.1600-065X.2010.00988.x (2011).
- 456 5 Weiss, W. R. *et al.* Cytotoxic T cells recognize a peptide from the circumsporozoite protein
457 on malaria-infected hepatocytes. *The Journal of experimental medicine* **171**, 763-773 (1990).
- 458 6 Romero, P. *et al.* Cloned cytotoxic T cells recognize an epitope in the circumsporozoite
459 protein and protect against malaria. *Nature* **341**, 323-326, doi:10.1038/341323a0 (1989).
- 460 7 Sano, G. *et al.* Swift development of protective effector functions in naive CD8(+) T cells
461 against malaria liver stages. *The Journal of experimental medicine* **194**, 173-180 (2001).
- 462 8 Cockburn, I. A. *et al.* Dendritic cells and hepatocytes use distinct pathways to process
463 protective antigen from plasmodium in vivo. *PLoS Pathog* **7**, e1001318,
464 doi:10.1371/journal.ppat.1001318 (2011).
- 465 9 Hollingdale, M. R., Leland, P., Leef, J. L., Leef, M. F. & Beaudoin, R. L. Serological reactivity of
466 in vitro cultured exoerythrocytic stages of Plasmodium berghei in indirect
467 immunofluorescent or immunoperoxidase antibody tests. *Am J Trop Med Hyg* **32**, 24-30
468 (1983).
- 469 10 Silvie, O., Briquet, S., Muller, K., Manzoni, G. & Matuschewski, K. Post-transcriptional
470 silencing of UIS4 in Plasmodium berghei sporozoites is important for host switch. *Molecular*
471 *microbiology* **91**, 1200-1213, doi:10.1111/mmi.12528 (2014).
- 472 11 Bertolino, P. & Bowen, D. G. Malaria and the liver: immunological hide-and-seek or
473 subversion of immunity from within? *Frontiers in microbiology* **6**, 41,
474 doi:10.3389/fmicb.2015.00041 (2015).

- 475 12 Thomson, A. W. & Knolle, P. A. Antigen-presenting cell function in the tolerogenic liver
476 environment. *Nat Rev Immunol* **10**, 753-766, doi:10.1038/nri2858 (2010).
- 477 13 Bertolino, P., Bowen, D. G., McCaughan, G. W. & Fazekas de St Groth, B. Antigen-specific
478 primary activation of CD8+ T cells within the liver. *Journal of immunology* **166**, 5430-5438
479 (2001).
- 480 14 Mueller, A. K. *et al.* Plasmodium liver stage developmental arrest by depletion of a protein at
481 the parasite-host interface. *Proceedings of the National Academy of Sciences of the United*
482 *States of America* **102**, 3022-3027, doi:10.1073/pnas.0408442102 (2005).
- 483 15 Feliu, V. *et al.* Location of the CD8 T cell epitope within the antigenic precursor determines
484 immunogenicity and protection against the *Toxoplasma gondii* parasite. *PLoS Pathog* **9**,
485 e1003449, doi:10.1371/journal.ppat.1003449 (2013).
- 486 16 Spielmann, T., Ferguson, D. J. & Beck, H. P. etramps, a new *Plasmodium falciparum* gene
487 family coding for developmentally regulated and highly charged membrane proteins located
488 at the parasite-host cell interface. *Molecular biology of the cell* **14**, 1529-1544,
489 doi:10.1091/mbc.E02-04-0240 (2003).
- 490 17 Mac-Daniel, L. *et al.* Local immune response to injection of *Plasmodium* sporozoites into the
491 skin. *Journal of immunology* **193**, 1246-1257, doi:10.4049/jimmunol.1302669 (2014).
- 492 18 Rai, D., Pham, N. L., Harty, J. T. & Badovinac, V. P. Tracking the total CD8 T cell response to
493 infection reveals substantial discordance in magnitude and kinetics between inbred and
494 outbred hosts. *Journal of immunology* **183**, 7672-7681, doi:10.4049/jimmunol.0902874
495 (2009).
- 496 19 Schmidt, N. W., Butler, N. S., Badovinac, V. P. & Harty, J. T. Extreme CD8 T cell requirements
497 for anti-malarial liver-stage immunity following immunization with radiation attenuated
498 sporozoites. *PLoS Pathog* **6**, e1000998, doi:10.1371/journal.ppat.1000998 (2010).
- 499 20 Lau, L. S. *et al.* CD8+ T cells from a novel T cell receptor transgenic mouse induce liver-stage
500 immunity that can be boosted by blood-stage infection in rodent malaria. *PLoS Pathog* **10**,
501 e1004135, doi:10.1371/journal.ppat.1004135 (2014).

- 502 21 Guebre-Xabier, M., Schwenk, R. & Krzych, U. Memory phenotype CD8(+) T cells persist in
503 livers of mice protected against malaria by immunization with attenuated Plasmodium
504 berghei sporozoites. *Eur J Immunol* **29**, 3978-3986, doi:10.1002/(SICI)1521-
505 4141(199912)29:12<3978::AID-IMMU3978>3.0.CO;2-0 (1999).
- 506 22 Fernandez-Ruiz, D. *et al.* Liver-Resident Memory CD8(+) T Cells Form a Front-Line Defense
507 against Malaria Liver-Stage Infection. *Immunity* **45**, 889-902,
508 doi:10.1016/j.immuni.2016.08.011 (2016).
- 509 23 Montagna, G. N. *et al.* Antigen export during liver infection of the malaria parasite augments
510 protective immunity. *mBio* **5**, e01321-01314, doi:10.1128/mBio.01321-14 (2014).
- 511 24 Coppi, A. *et al.* The malaria circumsporozoite protein has two functional domains, each with
512 distinct roles as sporozoites journey from mosquito to mammalian host. *The Journal of*
513 *experimental medicine* **208**, 341-356, doi:10.1084/jem.20101488 (2011).
- 514 25 Hafalla, J. C., Sano, G., Carvalho, L. H., Morrot, A. & Zavala, F. Short-term antigen
515 presentation and single clonal burst limit the magnitude of the CD8(+) T cell responses to
516 malaria liver stages. *Proceedings of the National Academy of Sciences of the United States of*
517 *America* **99**, 11819-11824, doi:10.1073/pnas.182189999 (2002).
- 518 26 de Cassan, S. C. *et al.* The requirement for potent adjuvants to enhance the immunogenicity
519 and protective efficacy of protein vaccines can be overcome by prior immunization with a
520 recombinant adenovirus. *Journal of immunology* **187**, 2602-2616,
521 doi:10.4049/jimmunol.1101004 (2011).
- 522 27 Cohen, J., Nussenzweig, V., Nussenzweig, R., Vekemans, J. & Leach, A. From the
523 circumsporozoite protein to the RTS, S/AS candidate vaccine. *Human vaccines* **6**, 90-96
524 (2010).
- 525 28 Rts, S. C. T. P. Efficacy and safety of RTS,S/AS01 malaria vaccine with or without a booster
526 dose in infants and children in Africa: final results of a phase 3, individually randomised,
527 controlled trial. *Lancet* **386**, 31-45, doi:10.1016/S0140-6736(15)60721-8 (2015).

- 528 29 Iwanaga, S., Kaneko, I., Kato, T. & Yuda, M. Identification of an AP2-family protein that is
529 critical for malaria liver stage development. *PLoS One* **7**, e47557,
530 doi:10.1371/journal.pone.0047557 (2012).
- 531 30 Muller, K., Matuschewski, K. & Silvie, O. The Puf-family RNA-binding protein Puf2 controls
532 sporozoite conversion to liver stages in the malaria parasite. *PLoS One* **6**, e19860,
533 doi:10.1371/journal.pone.0019860 (2011).
- 534 31 Zhang, M., Mishra, S., Sakthivel, R., Fontoura, B. M. & Nussenzweig, V. UIS2: A Unique
535 Phosphatase Required for the Development of Plasmodium Liver Stages. *PLoS Pathog* **12**,
536 e1005370, doi:10.1371/journal.ppat.1005370 (2016).
- 537 32 Tarun, A. S. *et al.* A combined transcriptome and proteome survey of malaria parasite liver
538 stages. *Proceedings of the National Academy of Sciences of the United States of America* **105**,
539 305-310, doi:10.1073/pnas.0710780104 (2008).
- 540 33 Lin, J. W. *et al.* The subcellular location of ovalbumin in Plasmodium berghei blood stages
541 influences the magnitude of T-cell responses. *Infection and immunity* **82**, 4654-4665,
542 doi:10.1128/IAI.01940-14 (2014).
- 543 34 Douglas, A. D. *et al.* The blood-stage malaria antigen PfRH5 is susceptible to vaccine-
544 inducible cross-strain neutralizing antibody. *Nat Commun* **2**, 601, doi:10.1038/ncomms1615
545 (2011).
- 546 35 Osier, F. H. *et al.* New antigens for a multicomponent blood-stage malaria vaccine. *Sci Transl*
547 *Med* **6**, 247ra102, doi:10.1126/scitranslmed.3008705 (2014).
- 548 36 Kapulu, M. C. *et al.* Comparative assessment of transmission-blocking vaccine candidates
549 against Plasmodium falciparum. *Sci Rep* **5**, 11193, doi:10.1038/srep11193 (2015).
- 550 37 Potocnjak, P., Yoshida, N., Nussenzweig, R. S. & Nussenzweig, V. Monovalent fragments
551 (Fab) of monoclonal antibodies to a sporozoite surface antigen (Pb44) protect mice against
552 malarial infection. *The Journal of experimental medicine* **151**, 1504-1513 (1980).
- 553 38 Tsuji, M., Mattei, D., Nussenzweig, R. S., Eichinger, D. & Zavala, F. Demonstration of heat-
554 shock protein 70 in the sporozoite stage of malaria parasites. *Parasitology research* **80**, 16-
555 21 (1994).

556 39 Janse, C. J. *et al.* High efficiency transfection of *Plasmodium berghei* facilitates novel
557 selection procedures. *Mol Biochem Parasitol* **145**, 60-70,
558 doi:10.1016/j.molbiopara.2005.09.007 (2006).
559

560 **Acknowledgements**

561 S.J.D is a Jenner Investigator, Lister Institute Research Prize Fellow and Wellcome
562 Trust Senior Fellow (106917/Z/15/Z). K.Matuschewski was supported by the Max Planck
563 Society and grants from the European Commission (EviMalaR Network of Excellence #34)
564 and the Chica and Heinz Schaller Foundation. O.S. was funded in part by the Laboratoire
565 d'Excellence ParaFrap (ANR-11-LABX-0024). J.C.R.H. was funded by grants from The
566 Royal Society (University Research Fellowship UF0762736/UF120026 and Project Grant
567 RG130034) and the National Centre for the Replacement, Refinement & Reduction of
568 Animals in Research (Project Grant NC/L000601/1). The funders had no role in study
569 design, data collection and analysis, decision to publish, or preparation of the manuscript.

570

571

572 **Author contributions**

573 K.Matuschewski, O.S. and J.C.R.H. designed the experiments; O.S. generated the
574 transgenic parasites CSP^{SIINFEKL} and UIS4^{SIINFEKL}; K.Müller, M.P.G., O.S. and J.C.R.H.
575 performed experiments and analysed data; A.R.-S., A.V.S.H. and S.J.D. provided the
576 adenovirus AdOVA; M.P.G. and J.C.R.H. wrote the paper; all authors commented and
577 revised the manuscript.

578

579

580 **Competing interests**

581 A.R.-S., A.V.S.H. and S.J.D. are named inventors on patent applications relating to
582 malaria vaccines, adenovirus vaccines and immunisation regimens.

583 **FIGURE LEGENDS**

584 **Figure 1: Generation and characterisation of recombinant CSP^{SIINFEKL} and UIS4^{SIINFEKL}**

585 ***P. berghei* parasites.**

586 *Pb* parasites expressing the CD8+ T cell epitope of ovalbumin, SIINFEKL, in the
587 context of CSP or UIS4 were generated using double homologous recombination. **(a)** To
588 generate CSP^{SIINFEKL}, SIINFEKL replaced amino acids SYIPSAEK in CSP. To generate
589 UIS4^{SIINFEKL}, SIINFEKL was adjoined to the carboxyl-terminus of the UIS4 protein. **(b)**
590 Sporozoite immunofluorescent antibody staining of WT, CSP^{SIINFEKL} or UIS4^{SIINFEKL}
591 sporozoites after gliding on BSA-coated glass slides. Shown are microscopic images of the
592 respective sporozoites that were stained with anti-CSP (green), anti-UIS4 (red) and nuclear
593 stain Hoechst 33342 (blue). Scale bars, 10µm. The numbers show mean percentage (±SD)
594 of sporozoites with trails assessed from ≥220 sporozoites. **(c)** Fluorescent-microscopic
595 images of EEF-infected Huh7 hepatoma cells. 24 and 48 hours after infection with WT,
596 CSP^{SIINFEKL} or UIS4^{SIINFEKL} sporozoites, the cells were fixed and stained with anti-UIS4 (red),
597 anti-HSP70 (green) and the nuclear stain Hoechst (blue). Scale bars: 10µm. The numbers
598 show mean numbers (±SD) of intracellular parasites counted from ≥200 EEFs.

599

600 **Figure 2: Kinetics of CD8+ T cell responses induced by transgenic parasites.**

601 **(a-b)** C57BL/6 mice (up to 8 per group) received 2x10⁶ OT-I cells alone (diamonds)
602 or were additionally immunised with 10,000 γ-radiation attenuated WT (triangles), CSP^{SIINFEKL}
603 (orange squares) or UIS4^{SIINFEKL} (blue circles) sporozoites intravenously. **(a)** Flow cytometry
604 plots show the gating strategy for identifying K^b-SIINFEKL+ CD11a+ CD8+ T cells. **(b)**
605 Peripheral blood was obtained on days 4, 7, 14, 21, 42 and 88 after immunisation and
606 stained for K^b-SIINFEKL+ CD11a+ CD8+ T cells. Line graph shows mean values (±SEM)
607 from representative experiments (*, p<0.05; **, p<0.01; ***, p<0.001; Welch's t-test). **(c-g)**
608 C57BL/6 mice (n=4), which received 2x10⁶ CFSE-labelled OT-I splenocytes, were
609 immunised with 10,000 γ-radiation attenuated WT, CSP^{SIINFEKL} or UIS4^{SIINFEKL} sporozoites
610 intravenously. 5 days later, mice were sacrificed, spleens harvested and splenocytes
611 assessed for **(c)** CFSE dilution and stained *ex vivo* **(d-f)** for effector CD8+ T cell surface

612 markers. Shown are flow cytometry plots of K^b-SIINFEKL co-staining with markers of effector
613 phenotypes: **(d)** CD11a^{hi}, **(e)** CD62L^{lo}, **(f)** CD49d^{hi} and **(g)** the proliferation of CFSE-labelled
614 antigen experienced K^b-SIINFEKL+ CD11a+ CD8+ T cells.

615

616 **Figure 3: Sporozoite surface antigen induces a higher CD8+ T cell response than EEF**
617 **vacuolar membrane antigen in the spleen and liver.**

618 C57BL/6 mice (up to 5) received 2x10⁶ OT-I cells alone or were additionally
619 immunised with 10,000 γ -radiation attenuated WT, CSP^{SIINFEKL} or UIS4^{SIINFEKL} sporozoites
620 intravenously. Spleens and livers were harvested either at day 14 or day 42. Proportions and
621 numbers of **(a-c)** K^b-SIINFEKL+ CD8+ T cells were enumerated or **(d-f)** IFN- γ -secreting
622 CD8+ T cells following restimulation *ex vivo* with SIINFEKL peptide were quantified. Flow
623 cytometry plots show representative percentages of CD8+ T cells co-stained with CD11a
624 and **(a)** K^b-SIINFEKL or **(d)** IFN- γ . The upper panel of bar charts **(b, e)** show the percentage
625 of co-stained CD8+ T cells and the lower panel **(c, f)** the absolute cell counts. Bar charts
626 show mean values (\pm SEM) from representative experiments (*, p<0.05; **, p<0.01; ***,
627 p<0.001; one-way ANOVA with Tukey's multiple comparison test).

628

629 **Figure 4: OT-I cells are not required to detect SIINFEKL-specific CD8+ T cell**
630 **responses.**

631 C57BL/6 mice (3-6 per group) received 10,000 γ -radiation attenuated WT,
632 CSP^{SIINFEKL} or UIS4^{SIINFEKL} sporozoites, either **(a-c)** intravenously or **(d-f)** intradermally.
633 Additional control mice did not receive sporozoites. Spleens and livers were harvested either
634 at day 14 or day 42, and IFN- γ -secreting lymphocytes following restimulation *ex vivo* with
635 SIINFEKL peptide were quantified. Flow cytometry plots show representative percentages of
636 CD8+ T cells co-stained with IFN- γ and CD11a **(a, d)**. The upper panel of bar charts **(b, e)**
637 show the percentage of CD11a+ IFN- γ + CD8+ T cells and the lower panel **(c, f)** the absolute
638 cell counts. Bar charts show mean values (\pm SEM) from representative experiments (*,
639 p<0.05; **, p<0.01; ***, p<0.001; one-way ANOVA with Tukey's multiple comparison test).

640

641 **Figure 5: Increasing antigen dose does not improve antigen-specific CD8+ T cell**
642 **responses to an EEF vacuolar membrane protein.**

643 C57BL/6 mice (4 per group) received an intravenous dose of 8,000 γ -radiation
644 attenuated CSP^{SIINFEKL} or UIS4^{SIINFEKL} sporozoites or 64,000 γ -radiation attenuated
645 UIS4^{SIINFEKL} sporozoites. Spleens and livers were harvested at day 12 and IFN- γ -secreting
646 lymphocytes following restimulation *ex vivo* with SIINFEKL peptide were quantified. **(a)** Flow
647 cytometry plots show representative CD8+ T cells co-stained with IFN- γ and CD11a. **(b)** The
648 upper panel of bar charts show the percentage of CD11a+ IFN- γ + CD8+ T cells and the
649 lower panel the absolute cell counts. Bar charts show mean values (\pm SEM) from
650 representative experiments (***, $p < 0.001$; one-way ANOVA with Tukey's multiple
651 comparison test).

652

653 **Figure 6: Sporozoite surface and EEF vacuolar membrane antigens are presented to**
654 **vaccine-induced CD8+ T cells for killing, leading to sterile protection.**

655 Mice received 1×10^8 ifu recombinant AdHu5 expressing whole ovalbumin (AdOVA)
656 and/or 2×10^6 OT-I splenocytes. **(a)** Flow cytometry and **(b)** scatter plots represent CD8+ T
657 cells derived from peripheral blood co-stained with IFN- γ and CD11a, following *ex vivo*
658 restimulation with SIINFEKL. **(c)** Protective efficacy as measured by quantitative real-time
659 PCR. Groups of mice (up to 11 per group) were vaccinated as described and challenged 19
660 days later with 10,000 WT, CSP^{SIINFEKL} or UIS4^{SIINFEKL} sporozoites. 42 hours later livers were
661 removed and parasite load was assessed by qPCR. Plots show the relative parasite load of
662 mice in each condition (**, $p < 0.01$; Mann-Whitney U test). **(d)** Proportion of sterile protection
663 after immunization. Mice (8 per group) were vaccinated as described and were challenged
664 with 1,000 WT, CSP^{SIINFEKL} or UIS4^{SIINFEKL} sporozoites. Data for **a-d** are representative of two
665 experiments performed with scatter plots showing mean values (\pm SEM).

666

667 SUPPLEMENTARY EXPERIMENTAL PROCEDURES

668 **Generation of CSP^{SIINFEKL} and UIS4^{SIINFEKL} transgenic *P. berghei* parasite lines**

669 B3D-CSP^{SIINFEKL} plasmid was assembled by successive cloning of three fragments, CSP-C,
670 CSP-B and CSP-A, obtained by PCR amplification from *P. berghei* ANKA genomic DNA
671 followed by restriction enzyme digestion. These fragments correspond respectively to a 3'
672 homology region downstream of CSP (CSP-C, 0.7 kb), a fragment comprising the CSP ORF
673 downstream of the SYIPSAEKI epitope followed by the CSP 3' UTR (CSP-B, 0.8 kb) and a
674 fragment comprising a 5' promoter region followed by the CSP modified ORF where the
675 SYIPSAEK coding sequence has been replaced by a SIINFEKL coding sequence (CSP-A,
676 1.8 kb). The resulting B3D-CSP^{SIINFEKL} plasmid, containing the *Toxoplasma gondii*
677 dihydrofolate reductase/thymidylate synthase (*TgDHFR/TS*) pyrimethamine resistance
678 cassette flanked by CSP-A and CSP-B on one side, and CSP-C on the other, was linearized
679 with *NotI* and *SacII* before transfection. Integration of the construct after double crossover
680 homologous recombination results in replacement of the WT CSP gene by a modified copy
681 containing the SIINFEKL coding sequence instead of the SYIPSAEKI coding sequence. The
682 B3D-UIS4^{SIINFEKL} plasmid was assembled by successive cloning of three fragments, UIS4-A,
683 UIS4-B and UIS4-C, obtained by PCR amplification from *P. berghei* ANKA genomic DNA
684 followed by restriction enzyme digestion. These fragments correspond respectively to a
685 fragment comprising a 5' upstream sequence followed by the UIS4 entire ORF fused in frame
686 to the SIINFEKL coding sequence (UIS4-A, 1.2 kb), to the UIS4 3' UTR sequence (UIS4-B,
687 0.6 kb) and to a 3' homology region downstream of UIS4 (UIS4-C, 0.9 kb). The resulting B3D-
688 UIS4^{SIINFEKL} plasmid, containing the *TgDHFR/TS* pyrimethamine resistance cassette flanked
689 by UIS4-A and UIS4-B on one side, and UIS4-C on the other, was linearized with *SacII* and
690 *KpnI* before transfection. Integration of the construct after double crossover homologous
691 recombination results in replacement of the WT UIS4 gene by a modified copy containing the
692 SIINFEKL coding sequence just upstream of a STOP codon. *P. berghei* CSP^{SIINFEKL} and
693 UIS4^{SIINFEKL} parasites were generated by transfection of *P. berghei* ANKA with linearized B3D-
694 CSP^{SIINFEKL} and B3D-UIS4^{SIINFEKL} plasmids, respectively. Purified schizonts of WT *P. berghei*
695 ANKA (clone c15cy1) were transfected with 5-10µg of linearized plasmid by electroporation

696 using the AMAXA Nucleofector™ device (program U33), as described³⁹, and immediately
697 injected intravenously in the tail vein of a mouse. The day after transfection, pyrimethamine
698 (70 mg/l) was administrated in the mouse drinking water, for selection of transgenic parasites.
699 Transgenic clones were isolated after limiting dilution and injection into mice. Correct
700 integration of the constructs and purity of the transgenic lines was verified by analytical PCR
701 using primer combinations specific for the unmodified CSP or UIS4 locus, and for the 5' and
702 3' recombination events. All primers used in this study are indicated in Table S1.

703

704

705 SUPPLEMENTARY FIGURE LEGENDS

706 **Suppl. Figure 1: Generation of transgenic CSP^{SIINFEKL} and UIS4^{SIINFEKL} *P. berghei* lines**

707 *Plasmodium berghei* parasites expressing the CD8+ T cell epitope of ovalbumin,
708 SIINFEKL, in the context of CSP or UIS4 were generated using double homologous
709 recombination, combining drug-resistance selection (through incorporation of the *dhfr/ts* gene
710 from *Toxoplasma gondii*) and cloning by limiting dilution to select for correctly recombined
711 parasites. **(a,b)** Diagrams illustrate the reverse genetics strategy. **(a)** In CSP^{SIINFEKL} SIINFEKL
712 replaces the immunodominant CD8+ T cell epitope SYIPSAEK(I) of CSP. **(b)** In UIS4^{SIINFEKL}
713 SIINFEKL is adjoined to the carboxyl-terminus of the UIS4 protein. Purified schizonts of WT
714 *P. berghei* ANKA were transfected with linearized plasmid by electroporation as described³⁹,
715 and immediately injected intravenously in the tail vein of a mouse. The day after transfection,
716 pyrimethamine (70 mg/l) was orally administered in the drinking water for selection of
717 transgenic parasites. Transgenic clones were generated in mice by *in vivo* cloning by limiting
718 dilution. Correct integration of the constructs and purity of the transgenic lines was verified by
719 diagnostic PCR using primer combinations specific for the unmodified *CSP* or *UIS4* locus, and
720 for the 5' and 3' recombination events as indicated by lines, arrows and expected fragment
721 sizes. **(c)** Oocyst midgut infectivity of mosquitoes infected with WT, CSP^{SIINFEKL} or UIS4^{SIINFEKL}.
722 The mean percentage (\pm SD) of infected midguts was enumerated 10-14 days after infection
723 (n = at least 7 infections). **(d)** Salivary glands were isolated from WT, CSP^{SIINFEKL} or UIS4^{SIINFEKL}
724 infected mosquitoes and mean sporozoite numbers (\pm SD) were enumerated between 18-23

725 days after infection (n= at least 13 infections).

726

727 **Suppl. Figure 2: Sporozoite surface antigen induces a greater effector CD8+ T cell**
728 **phenotype than EEF vacuolar membrane antigen.**

729 C57BL/6 mice (up to 5 per group) received 2×10^6 OT-I cells alone or were additionally
730 immunised with 10,000 γ -radiation attenuated WT, CSP^{SIINFEKL} or UIS4^{SIINFEKL} sporozoites
731 intravenously. Spleens and livers were harvested either 14 or 42 days later, and proportions
732 of CD8+ T cells expressing effector surface markers were quantified. Flow cytometry plots
733 show representative percentages of CD8+ T cells co-staining K^b-SIINFEKL and markers of
734 effector phenotype (CD11a^{hi}, CD49d^{hi}, CD62L^{lo}, CD44^{hi}).

735

736 **Suppl. Figure 3: Antigen experienced SIINFEKL-specific CD8+ T cells also produce**
737 **TNF- α and IL-2.**

738 C57BL/6 mice (up to 5 per group) received 2×10^6 OT-I cells alone or were additionally
739 immunised with 10,000 γ -radiation attenuated WT, CSP^{SIINFEKL} or UIS4^{SIINFEKL} sporozoites
740 intravenously. Spleens and livers were harvested either 14 or 42 days after immunisation and
741 lymphocytes restimulated *ex vivo* with SIINFEKL peptide at 10 μ g/ml per well for 5-6 hours.
742 The upper panel of bar charts show the percentage of CD11a+ TNF- α secreting CD8+ T cells,
743 the bottom panel CD11a+ IL-2 secreting CD8+ T cells. This is a representation of one
744 experiment from two experiments performed. Bar charts show mean values (\pm SEM) from
745 representative experiments (*, p<0.05, **, p<0.01, ***, p<0.001; one-way ANOVA with Tukey's
746 multiple comparison test).

747

748 **Suppl. Table 1: Primers used to generate plasmids and genotype parasites**

749

	Oligonucleotide	Sequence 5' → 3'
Production of B3D-CSP^{SIINFEKL} construct	CSP-A forward	ATAAGAATGCGGCCGCATGGTTATATTTTGTGCAATGCTAAAATGG
	CSP-A reverse	<u>CGGAATTC</u> TAGTATCAGTTTTTCAAAGTTGATTATACTATCGTCATTATTATTA TTTTTGTATTG
	CSP-B forward	<u>GGACTAGTGAATTC</u> GTAAACAGATCAGGGATAGTATCACAGAGG
	CSP-B reverse	CCG <u>CAATTG</u> TACAAAAATATTTTCGACAAAGGATAACG
	CSP-C forward	CCCA <u>AGCTT</u> TGGGAATCTATTTTACAATATATTTAAGGG
	CSP-C reverse	CGGGTACCCCGCGGTTATTGAAAAAGACACAAAATAGCTAG
Production of B3D-UIS4^{SIINFEKL} construct	UIS4-A forward	TCCC <u>CGCG</u> GATAGCTATATTTTATGGTTGATCCTTTCC
	UIS4-A reverse	<u>GGACTAGTTT</u> ACAGTTTTTCAAAGTTGATTATACTTATGTATGGGCCGAATGAT TTATTTTCC
	UIS4-B forward	<u>GGACTAGTTT</u> CATTATGAGTAGTGTAATTCAGAAAGAG
	UIS4-B reverse	CCG <u>GAAATTC</u> TATGTAAAAAGTTTGCATATACGGCTG
	UIS4-C forward	CCCA <u>AGCTT</u> AGTGAAATATAAATATGAATGGAAGCAGCC
	UIS4-C reverse	CGGGTAC <u>CAGCAG</u> CTAATGTCAATATATTTTATGCAC
Genotyping of transgenic parasites	TgDHFR forward	CGCATTATATGAGTTCATTTTACACAATCC
	OVA reverse	CTAGTTTACAGTTTTTCAAAGTTGATTATAC
	CSP WT forward	TGTGAACTTTTCCTTATTTATTACGATTATG
	CSP forward	test AATATGAGCAGCTTTTACTTTGTCCAGG
	CSP reverse	test ACGAATCGAAATAAGTTACTATTCGTGCC
	UIS4 forward	test TGGTTCTTAATATATTTTGGATACATGC
	UIS4 reverse	test CTCGTGCCTTTGTAGTAAAAATAAACC

750

751

752 Restriction sites in the primer sequences are underlined.

753

FIGURE 1

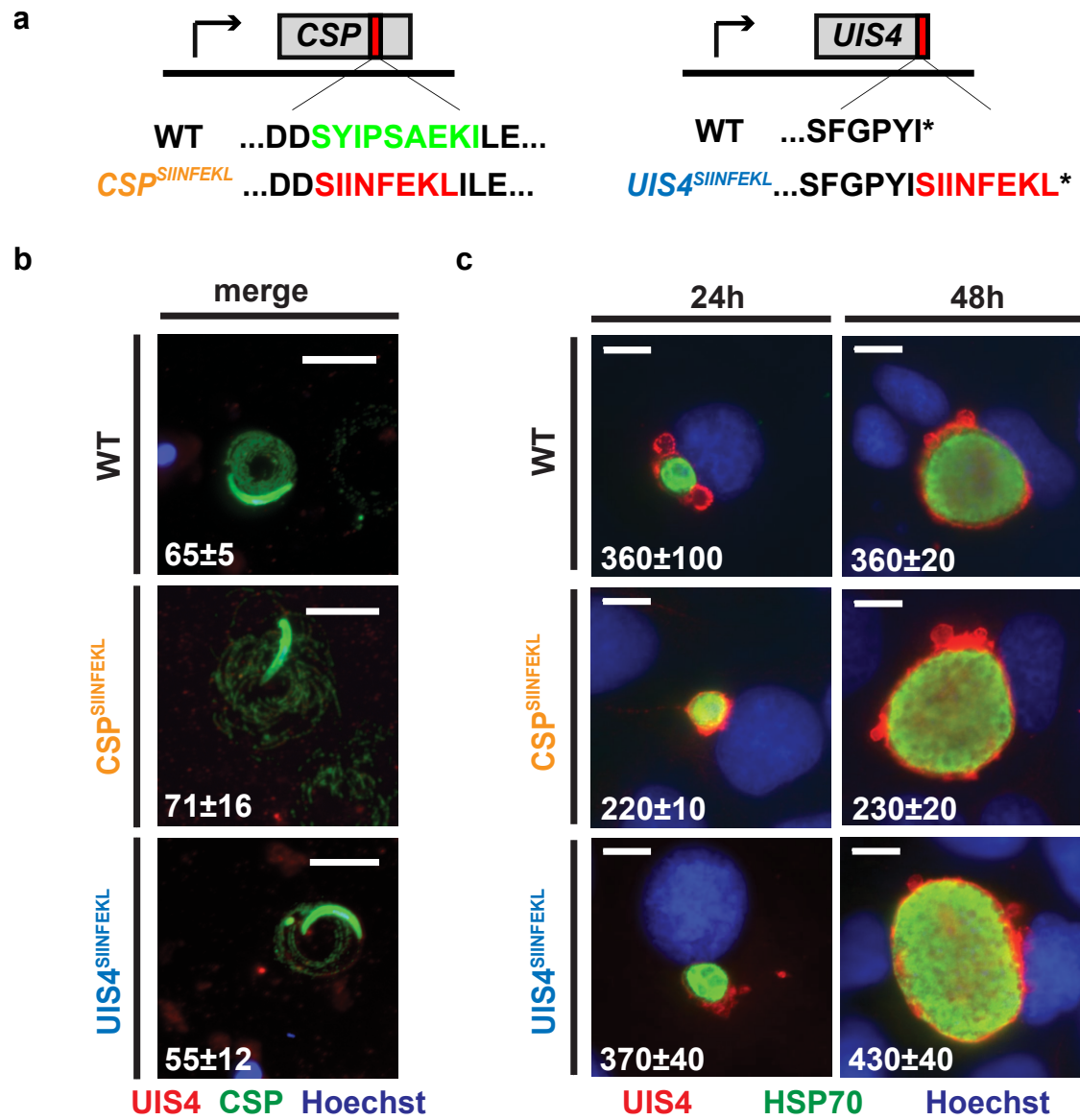


FIGURE 2

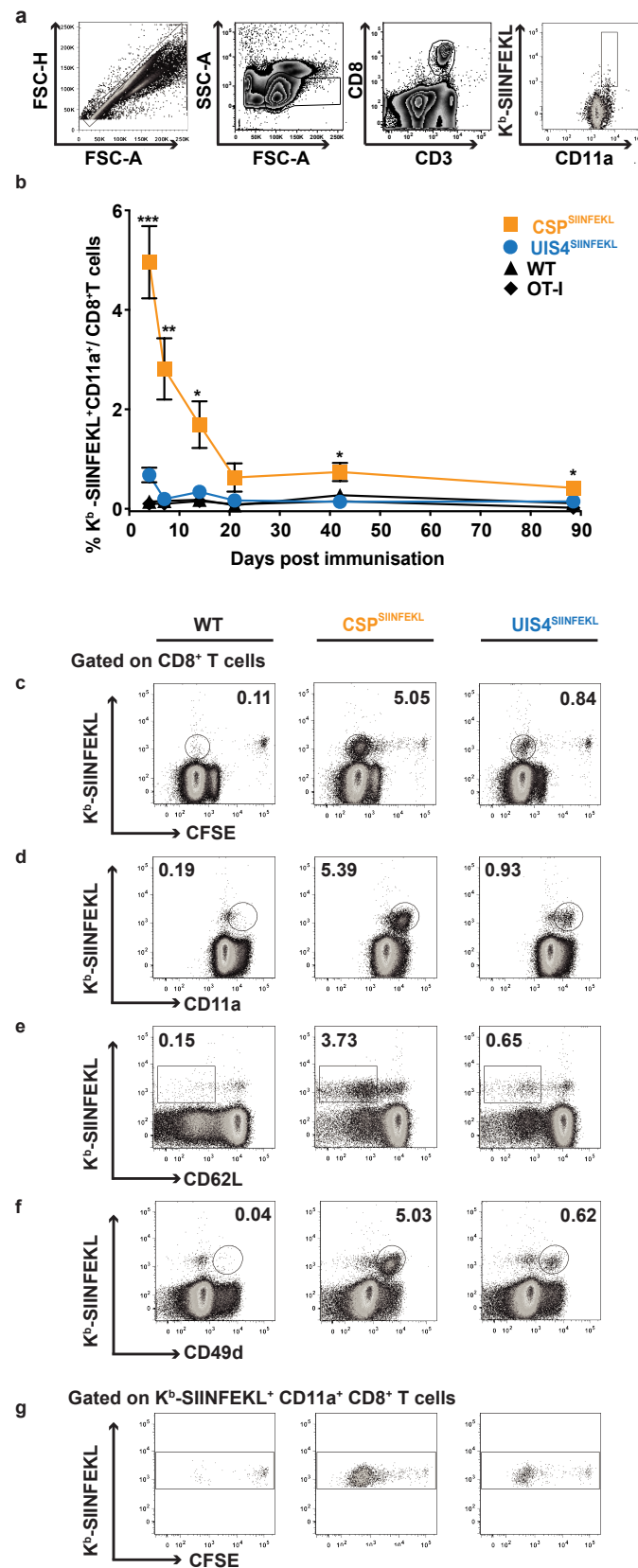


FIGURE 4

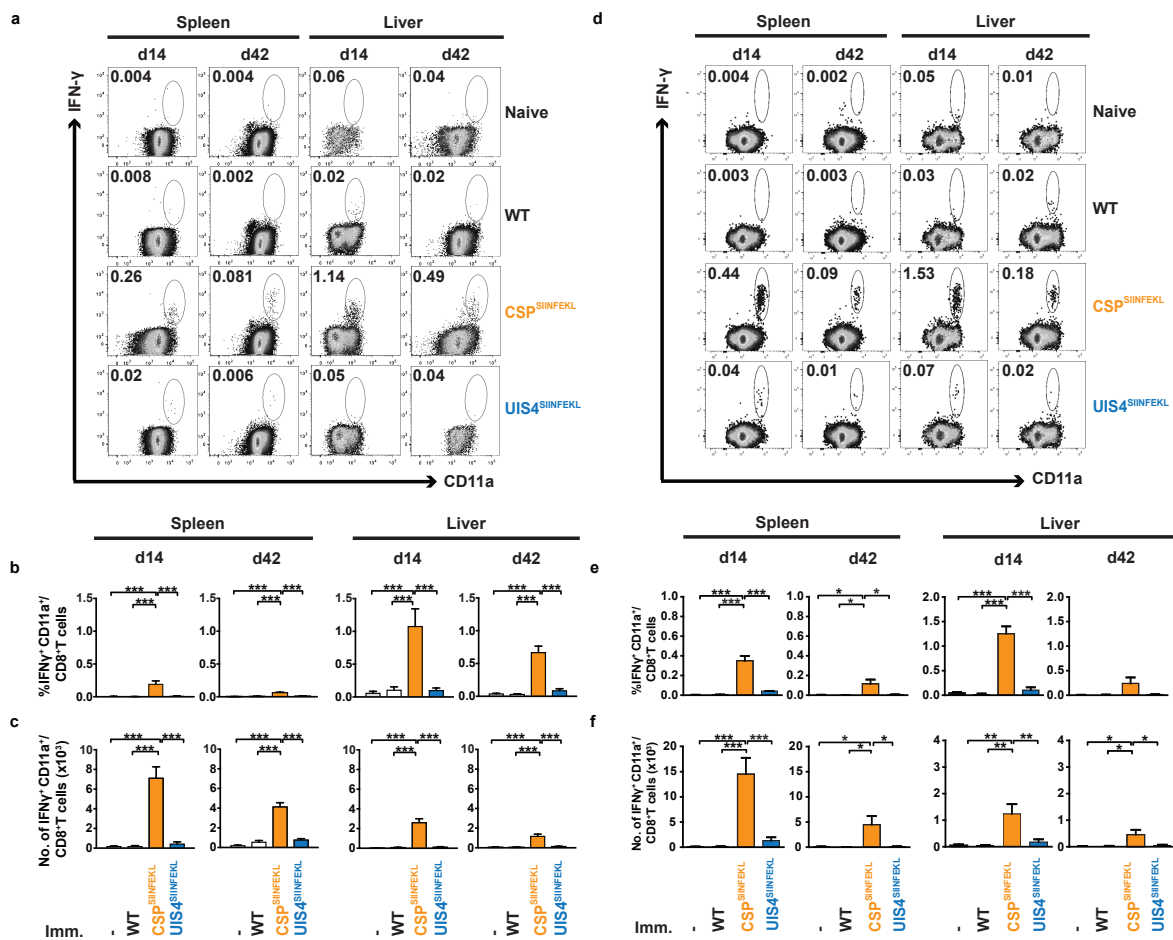


FIGURE 5

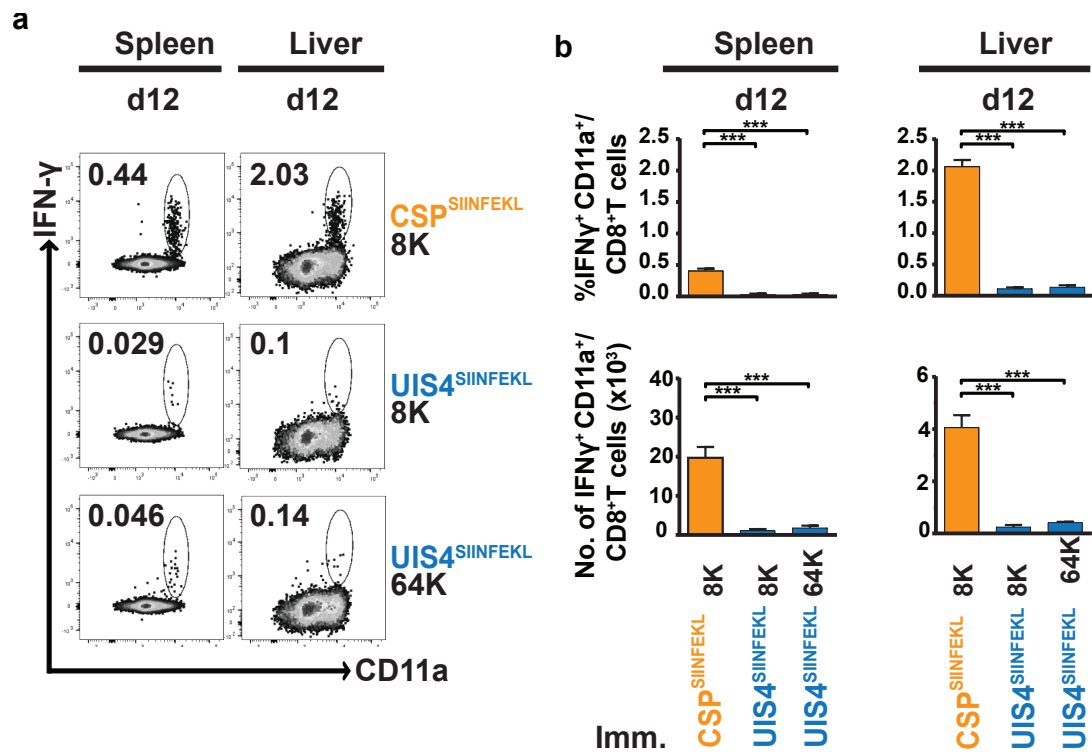


FIGURE 6

